Available online at www.sciencedirect.com
SCIENCE DIRECT
Trans. Nonferrous Met. Soc. China 16(2006) 1121−1128
Transactions of Nonferrous Metals Society of China
www.csu.edu.cn/ysxb/

Effect of large cold deformation on characteristics of age-strengthening of 2024 aluminum alloys

NING Ai-lin(宁爱林)[1,2], LIU Zhi-yi(刘志义)[1], ZENG Su-min(曾苏民)[1,2]

1. School of Materials Science and Engineering, Central South University, Changsha 410083, China;
2. Department of Mechanical Engineering, Shaoyang University, Shaoyang 422004, China

Received 1 December 2005; accepted 2 March 2006

Abstract: Effect of large cold deformation on the age-hardening characteristics of 2024 aluminum alloys was investigated. The results reveal: 1) the aging response is accelerated after large cold deformation, and the peak strength is attained after aging for 40 min; 2) double aging peaks can be found in the age-hardening curves, and the first peak appears when aged for 40 min. The corresponding peak tensile strength (σ_b) and elongation are up to 580 MPa and 9.2% respectively, the second peak appears when aged for 120 min, but the peak tensile strength (520 MPa) is lower than the first one; 3) in early stage of aging (＜40 min), elongation slightly increases from 8% with prolonging aging time of the alloy. Elongation markedly decreases to 2% after aging for 60 min, and shows a plateau with the prolonging of aging time on the age-elongation curve. It is indicated that the high density of dislocation introduced by large deformation accelerates the precipitation of GP zones and the aging response of the alloy. The first aging peak is due to the formation of GP zones and the deformation strengthening caused by the high density of dislocation. And the second peak present in the aging curve is attributed to the nucleation and growth of *S′* phase. The offset between dislocation density decreases and precipitation *S′*-phase finally results in the phenomenon of double aging peaks when aged at 190 ℃. Moreover, it is suggested that the formation of PFZ and coarse equilibrium phase accompanied by the precipitation of S′ phase decrease the elongation.

Key words: aluminum alloy; cold deformation; aging strengthening; mechanical properties

1 Introduction

Studies on thermomechanical treatment of aluminum alloy start from 1960s[1,2]. The thermo-mechanical treatment is divided into intermediate thermomechanical treatment(ITMT) and final thermo-mechanical treatment(FTMT) by Russo and his co-workers[3]. ITMT comprises high temperature precipitation of ancellary elements, which focuses on refining grain morphologies, modifying as-cast microstructures and depleting component segregation. FTMT including a low temperature age-hardening combines strengthening of deformation and precipitation. For the age-hardening aluminum alloys, the introduced dislocations can act as the superior nucleation site for the precipitates. Therefore the higher strength can be obtained after solution treatment. For example, 2XXX aluminum alloys are usually processed by T8 treatment. MCEVILY and his co-workers[2] studied Al-Zn-Mg alloys, and they found that cold work prior to aging could bring a small improvement to the tensile strength and could also improve fatigue properties and resistance to stress-corrosion cracking. In OSTERMANN's work[4], an increase of 25% in the 10^7 cycles-to-failure stress level in 7075 aluminum alloys was achieved by thermo-mechanical treatment. The thermomechanical treatment employing step-aging was studied by RUSSO et al[5], and better ductility and fracture toughness were obtained. RACK[6] and CHIA et al's[7] research indicated that a desirable microstructure for good fatigue properties is fine equiaxed grains with a uniform dislocation distribution, which is strongly locked by fine precipitates. JAHN and LUO's investigation[8] implied that pre-aging at 100 ℃ gave an improvement in tensile strength of 7475 aluminum alloys, but fatigue properties of the alloy obviously improved due to the pre-aging at room temperature.

Foundation item: Project(50571069) supported by the National Natural Science Foundation of China; Project(05A061) supported by the Department of Education of Hunan Province, China
Corresponding author: NING Ai-lin; Tel: +86-739-5431794; E-mail: nal57@163.com

In recent years, there are many investigations of thermomechanical treatment on 2XXX aluminum alloys [9−19]. CHATURVEDI et al[17] studied the effects of deformation on microstructures and properties of 2036 aluminum alloys after quenching treatment. A characteristic of double peaks phenomenon presents on aging curves in these alloys. However the studies of SINGH et al[18] and ZHAO et al[19] are different from CHATURVEDI and CHUNG, which shows a single peak on the age-hardening curve. For the main hardening phases of alloys used by CHATURVEDI with Cu-to-Mg ratio equal to 5.69 are θ' and S', and that of alloys used by SINGH and ZHAO with Cu-to-Mg ratio more than 8 is θ'. To understand the relationships between the aging characteristics and the components more clearly, in this study the aging characteristics of a 2024 aluminum alloy with a lower Cu-to-Mg ratio strengthened mainly by S' phase after cold deformation are investigated.

2 Experimental

The experimental sheets of 2024 aluminum alloy with a thickness of 20 mm were provided by Southwestern Aluminum Fabrication Plant, and the chemical composition of the alloy is listed in Table 1.

Table 1 Chemical composition of 2024 aluminum alloy (mass fraction, %)

Cu	Mg	Mn	Fe	Cr	Si	Al
4.12	1.43	0.54	0.13	0.12	0.11	Bal.

After quenching, the as-received materials were rolled down to 4 mm in thickness at 250 ℃ followed by solution treatment, then cold rolled to 2 mm, at last single-step aged. The solution treatment was performed on an electric resistance furnace with temperature fluctuation within ±1 ℃ controlled by a potential differential meter. In water quenching, samples were transferred to water within 5 s. Over-aging and single aging treatment were performed on a hot-air-circulating furnace with temperature fluctuation within ±1 ℃ controlled by mercury thermometer. Details of processing parameter are given in Table 2. Mechanical properties of different heat treatment samples(σ_b, $\sigma_{0.2}$ and δ_5) were measured on a CSS-4400 test machine. The fracture surfaces were examined using a KYKY-2800 scanning electron microscope. Dislocation structure, boundary configuration and structure of precipitation phases were investigated using an H-800 transmission electron microscope. Microstress was determined by X-ray diffraction.

3 Results

Fig.1 shows the tensile properties of samples under different aging conditions. It can be seen that mechanical properties of 2024 aluminum alloys are improved drastically after cold deformation, and the corresponding tensile strength and elongation (δ_5) are above 572 MPa and 9.1%, respectively.

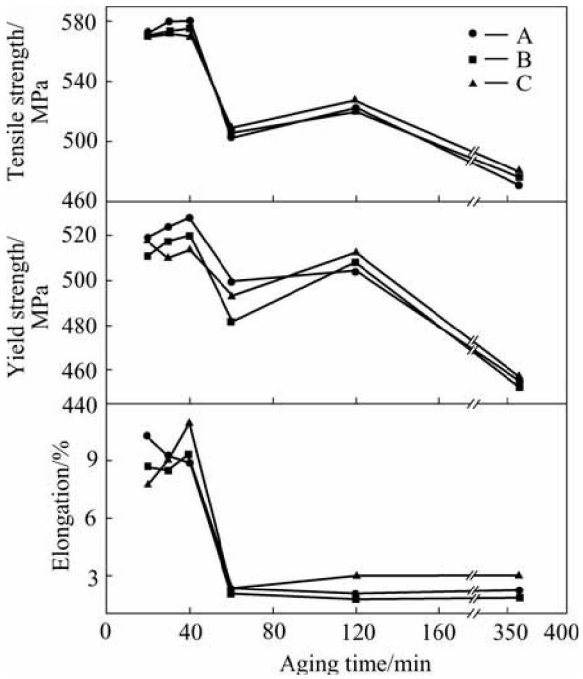

Fig.1 Mechanical properties for process A, B and C of 2024 aluminum alloy

The tensile strength (580 MPa) is obtained by optimal regime route B with 9.2% elongation, while σ_b and δ_5 of T62 treated 2024 aluminum alloys are 440 MPa and 5%, respectively. Fig.1 shows that the aging response of 2024 alloys is accelerated markedly after 50% cold deformation, and the peak strength of the alloys is obtained after aging for 40 min merely. It is shown that tensile strength and yield strength of all three routes exhibit double peaks characteristics on aging

Table 2 Processing parameters of 2024 aluminum alloy

Test process	Solution treatment	Overaging	Warm rolling	Solution and recrystallization	Cold rolling	Single stage aging (190 ℃)/min
A	470 ℃, 30 h	350 ℃, 6 h	250 ℃, 80%	470 ℃, 20 min	Room temperature, 50%	20, 30, 40, 60, 120, 360
B	470 ℃, 30 h	350 ℃, 6 h	250 ℃, 80%	470 ℃, 25 min	Room temperature, 50%	20, 30, 40, 60, 120, 360
C	470 ℃, 30 h	350 ℃, 6 h	250 ℃, 80%	470 ℃, 30 min	Room temperature, 50%	20, 30, 40, 60, 120, 360

strengthening curves. The first peak and the second peak are attained after aging for 40 min and 120 min at 190 ℃, respectively. The variations of elongation and strength have the same tendency when aged within the first peak with the lowest elongation more than 8% at a relatively high level, and the alloys exhibit a ductile facture behavior. The relatively low elongation about 2% remains constant as aging time prolongs, shaping a plateau in elongation curve, and the alloy shows a brittle fracture behavior.

Investigation by scanning electron microscopy indicates that there are many uniform deeper dimples on fracture surface of samples after aging for 40 min at 190 ℃, which shows a ductile fracture characteristic (Fig.2(a)). This fracture behavior is consistent with the aging curve of Fig.1 when aged for less than 40 min. There are fewer dimples on fracture surface of specimens aged for 60 and 360 min at 190 ℃ than aged for 40 min, showing a brittle fracture characteristic, corresponding to the low plastic deformation region of Fig.1 aged for more than 60 min, as shown in Figs.2(b) and (c). There is no shearing-plateau on fracture surface of samples when aged for 40 min at 190 ℃. But there are many shearing-plateaus on fracture surface of the specimen aged for 60 and 360 min at 190 ℃, as shown in Fig.3. Fig.4 also illustrates that the second phase particles are $S(Al_2CuMg)$ detected by electron probe, which locate at the sites of cracks, as shown in Fig.4.

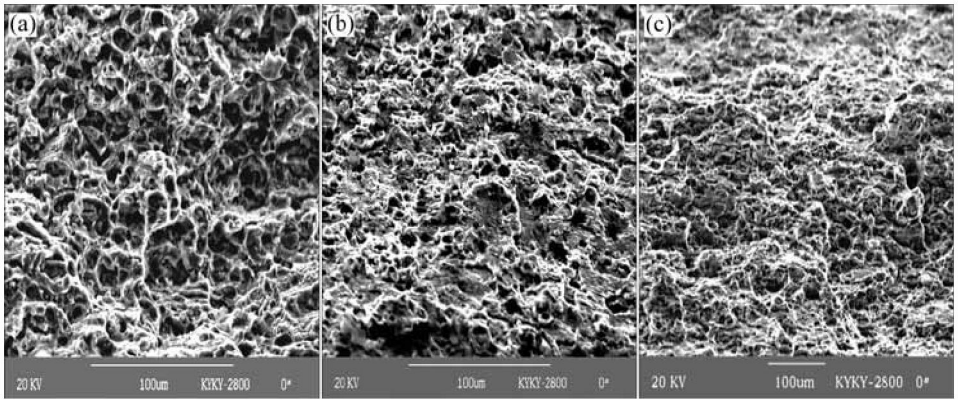

Fig.2 Tensile fracture morphologies of specimen aged for different times (route B): (a) 190 ℃, 40 min; (b) 190 ℃, 60 min; (c) 190 ℃, 360 min

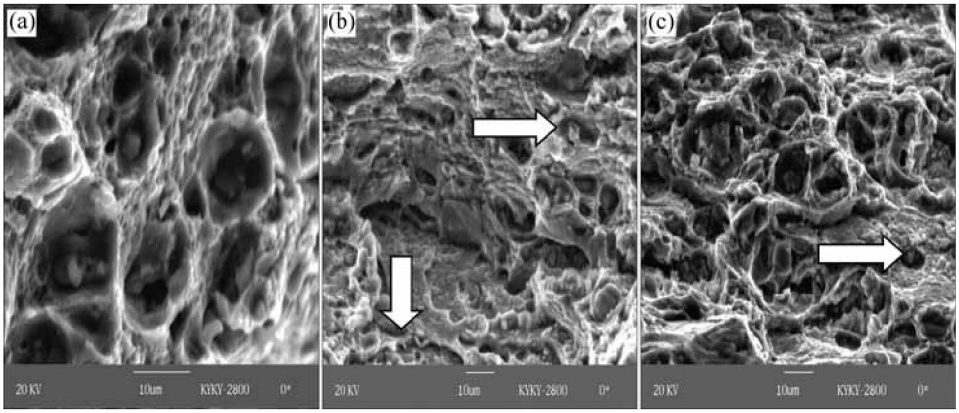

Fig.3 Tensile fracture morphologies of specimen aged for different time (route B): (a) 190 ℃, 40 min; (b) 190 ℃, 60 min; (c) 190 ℃, 360 min

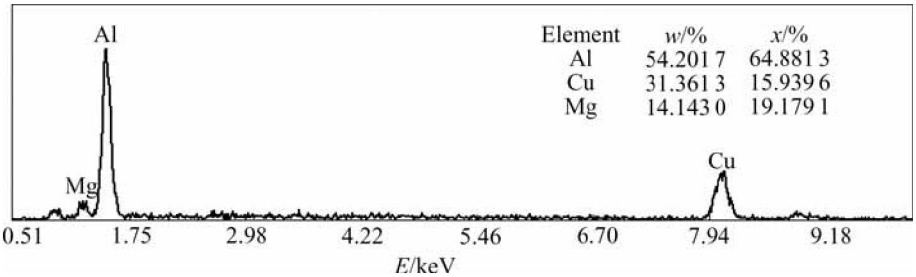

Fig.4 Second-phase particle component of fracture surface detected by electron probe

Investigation by TEM suggests that dislocation cells form in route B treated alloys when aged for 20 min. After aging for 30 min, the dislocation cells begin to grow. When aged for 60−360 min, the structure of dislocation cells disappears and is evolved to dislocation tangles (Fig.5). TEM observation also shows that there are no precipitates or precipitate-free zones (PFZ) in the alloys aged for 20 min and 30 min. After aging for 60 min, S' phase forms, and equilibrium phase S and PFZ also appear at grain boundaries, as shown in Fig.6.

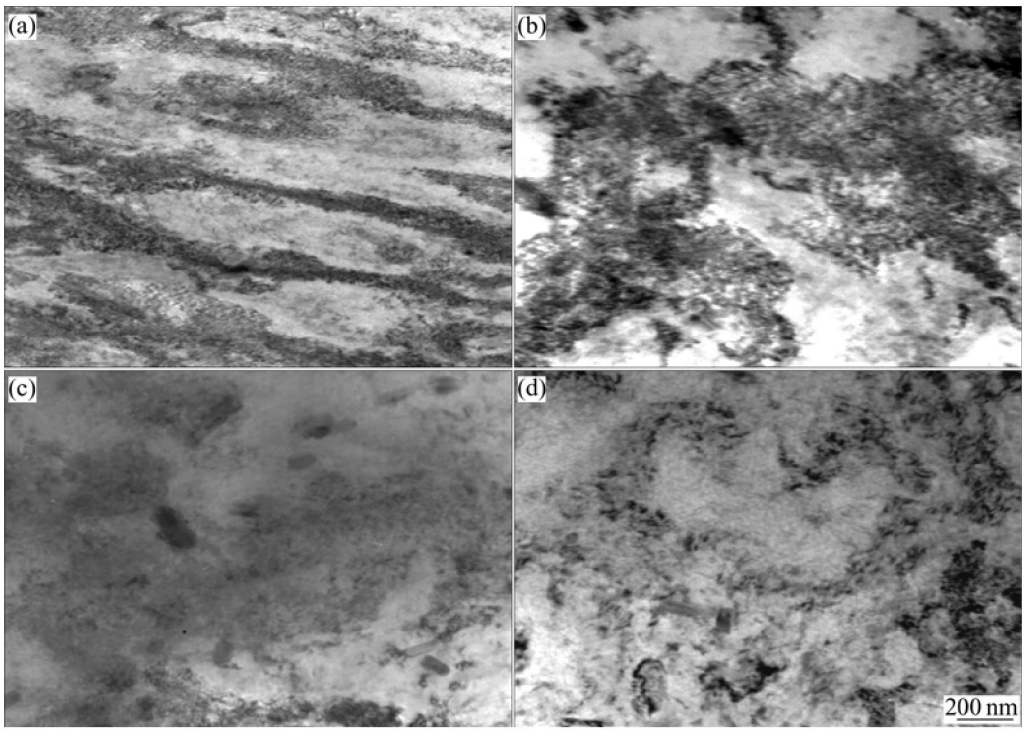

Fig.5 Dislocation structure of samples aged for different times (route B): (a) 190 ℃, 20 min; (b) 190 ℃, 30 min; (c) 190 ℃, 60 min; (d) 190 ℃, 360 min

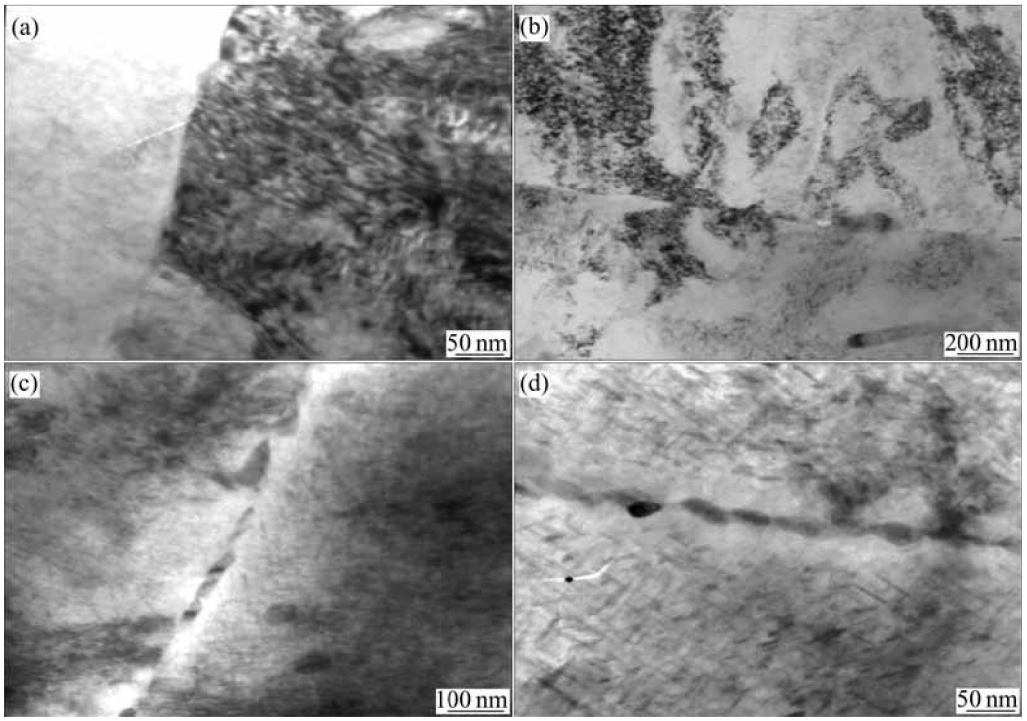

Fig.6 Microstructure at grain boundaries in specimens aged for different times (route B): (a) 190 ℃, 20 min; (b) 190 ℃, 30 min; (c) 190 ℃, 60 min; (d) 190 ℃, 360 min

Microstress reflecting distortion of crystal lattice was detected. The results show that microstress of specimen aged for 20 min has the lowest value, and the higher values of microstress are obtained in specimens aged for 30 min and 40 min. After aging for 60 min, the microstress begins to decrease, and the microstress reduces to the minimum after aging for 120 min and remains constant with prolonging aging time, as seen in Fig.7.

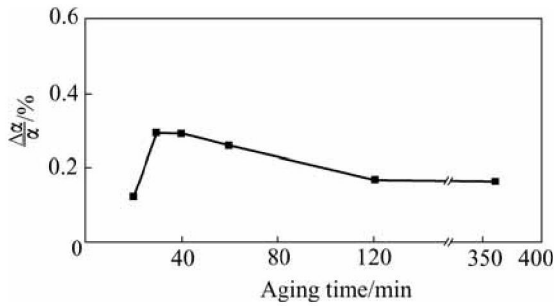

Fig.7 Microstress at different aging times

3 Analysis and discussion

3.1 Characteristics of age-strengthening

Tensile strength curves show that after cold deformation the aging response of the alloys is rapid. The tensile strength of the alloy reaches 573 MPa when aged for 20 min, then the strength increases slightly with aging time prolonging (Fig.1). The structure of the alloys under this aging condition is a typical one, which is composed of dislocation cells. It is suggested that dislocations induced by cold deformation recover to substructures during aging at 190 ℃ for 20 min. And an intense effect of deformation-hardening is achieved by introducing high density of dislocations. Meanwhile, the high density of dislocation can act as the channel of atomic diffusion, which accelerates the aging response by promoting the formation of G.P. zones. As we can see from the tendency of dislocations changing with the aging time that dislocation densities of the alloys gradually decrease with the prolonging aging time. It is suggested that effects of deformation decrease gradually with prolonging aging time. The strength of alloys would decrease in this process. However, Fig.1 shows the strength of aged alloys increases slightly after aging for 20 and 30 min. It is indicated that the increase of strength is due to the increase of GP zones or phase transformation, although no GP zones could be observed in the specimens. Main strengthening phase of the alloys used in present work with Cu-to-Mg ratios equal to 2.88 is *S*′. The precipitation sequence of this alloys[20−22] is SSS→GP Ⅰ zone→GP Ⅱ zone→*S*′→*S*. The precipitates are mainly GP Ⅰ zones and GP Ⅱ zones in the early stage of aging, so dislocation induced by cold deformation and GP zones are the main strengthening factors. Results of microstress indicate the lattice distortions of alloys aged for 30 and 40 min are higher than those of the alloys aged for 20 min (Fig.7). The high distortion is attributed to the increase of GP zones and the transformation of disc atom cluster GP Ⅰ zones to rod-like GP Ⅱ zones which are coherent with the matrix. As mentioned above, the increase of lattice distortion is due to the increase of GP zones and the transformation of GP Ⅰ zones to GP Ⅱ zones in the case of decrease of dislocation density. Therefore the strength reinforced by GP zones compensates the decrease of strength caused by the reduction of deformation strengthening, which causes a slight increase of strength from aging time 20 min to 40 min. Apparently, the peak strength of this stage is due to the combined strengthening effects caused by GP zone and cold plastic deformation.

When aged for 60 min, the strength of alloys is decreased obviously (Fig.1). By TEM observation, it is found that the structure of dislocation cell is annihilated and replaced by dislocation tangles (Fig.5(c)). It is obvious that the changes in the structure of dislocation mentioned above may result in the decrease of effect of deformation strengthening. Although *S*′ phase starts to precipitate (Fig.6(c)), the volume fraction of *S*′ precipitates is still relatively small, by which the effect of precipitation strengthening caused is not enough to compensate the decrease of strength led by drastic reduction of dislocation density. So the strength of the alloy presents a decreasing tendency. By analyzing the lattice distortion of aged samples, it can be seen that the lattice distortion still remains a high value when the dislocation cells disappear and dislocation density decrease drastically (Fig.7). This experimental fact may suggest that the *S*′ at this time is still under the condition of full coherence with matrix at early stage of precipitation. With prolonging aging time, *S*′ phase grows, the volume fraction of precipitates increases and the second peak of age-strengthening appears, as shown in Figs.1 and 6(c). It can be seen in Fig.1 that compared with the first peak of strengthening, the second one presents a relatively lower strength value of only 520 MPa, which is about 20 MPa higher than the strength of alloys when aging for 60 min. SILCOCK pointed out that strengthening in aging process of Al-Cu-Mg alloys with Cu-to-Mg ratio equal to 2.2 can be divided into two stages: one is GP zone strengthening stage and the other is *S*′ strengthening stage[23], which is consistent with the results in the present work. It is because of two stage of strengthening characteristic and effect of the introduced

strain hardening that the peak strength at first stage of strengthening reaches as high as 580 MPa. In the second stage, because the effect of strain hardening is lowered by S' phase, the strength only keeps at a peak value of 520 MPa, which is much lower than the first one. Meanwhile in spite of the annihilation of the effect of strain hardening, because S' phase starts to precipitate in the sample aged for 60 min, it still retains a high value of strength up to 500 MPa. So, in the case that the effect of strain hardening continues to decrease, the sample aged for 120 min only depends on the increase of volume fraction of S' phase to enhance the strength. The effect is limited and an amplitude of strength enhancement of only 20 MPa is presented. Consequently the decrease of strength at this stage can be attributed to decline of the effect of strain hardening. The enhancement of volume fraction of S' phase brings the second peak of age-strengthening, which is much lower than the first one because a small increase of strength is created by exclusive role of increase of volume fraction of S' precipitates in case that the effect of strain hardening is still at a relatively high level.

When compared the results in Refs.[17−19], it can be seen that the alloy strengthened mainly by θ' phase presents a characteristic of single peak of age-strengthening when being aged after large cold deformation. Those alloys strengthened by combined effect of θ' and S' phase or exclusive S′ phase in present work exhibit a characteristic of double peak of age-strengthening. By comparing the investigation results given by Refs. [17−19, 23−24], it is indicated that the aging response of the alloy mainly strengthened by θ' phase is faster than that by S′ phase, which suggests that θ' phase precipitates more rapidly than S' phase. The investigation work in Refs.[18, 19] indicates that the precipitation of θ' phase is consistent with the change of strain hardening with aging time due to more rapid precipitation rate of θ' phase, so that the curve of age-strengthening of the alloy presents a characteristic of single peak of strengthening. In spite of the fact mentioned above, the phenomenon that strength of the alloy gently changes with ageing time presented by Ref.[20] also obviously reflects the combined effects of two kind of strengthening process of strain hardening and age-strengthening. However the investigation in Ref.[18] and present work indicates that the response of strengthening of alloy gets behind the decrease in effect of strain hardening due to the slowness of precipitation of S' phase and shows a characteristic of double peak of age-strengthening.

3.2 Analysis on characteristic of elongation

Fig.1 shows a step-type behavior of elongation change with aging time. When the aging time is less than 40 min, the elongation that is all above 8% shows a tendency to increase slightly, and the sample shows a typical characteristic of dimple-type fracture (Figs.2(a), 3(b)). The elongation that changes flatly with ageing time is only about 2%, much lower than that of the sample aged for 40 min. When the aging time is more than 60 min, the sample exhibits many shear plateaus displaying low ductility on fracture surfaces (Figs.2(b) and (c), Figs.3(b) and (c)). Considering the mechanism of age-strengthening mentioned above, it can be seen that the factors of strengthening at this stage are strain-hardening and GP Ⅰ, Ⅱ zones strengthening. In the present work, the effect of strain strengthening is achieved by dislocation slip pinned by dislocation walls, and effect of strengthening caused by GP zones is accomplished by obstructing from incision of dislocation slip. TEM analysis shows that the microstructure in alloy aged for 20 and 30 min is a dislocation cell which grows with aging time prolonging, as shown in Figs.5(a) and (b). The result of distortion of crystal lattice indicates that the precipitate in alloy is GP Ⅰ of smaller distortion of crystal lattice when being aged for 20 min and GP Ⅱ of larger distortion of crystal lattice when being aged for 30 min. Because GP is incised by dislocation slip, at this stage of ageing, the essential obstruction of dislocation slip is the wall of dislocation cell. The size of dislocation cell therefore can be taken as unrestricted spacing for dislocation slip. The size of dislocation cell increases with ageing time prolonging at this stage, which means the enlargement of unstricted spacing for dislocation slip and enhancement of elongation of fractured samples. That is the reason why the elongation of alloy aged for less than 40 min in Fig.1 shows a tendency to slightly increase.

High magnification fractograph of alloys aged for more than 60 min shows a lot of shearing plateau on fracture surface (Figs.3(b) and (c)), and it could be seen that the shearing cracks initiate from the second phase marked by arrows in the figure. Detected by electron probe, the second phase in Fig.3 is Al-Cu-Mg with composition near Al_2CuMg as shown in Fig.4. TEM analysis indicates that the dislocation cell corresponding to this stage of ageing disappears, and S' phase precipitates instead, as shown in Figs.5(c) and (d), Figs.6(c) and (d). Obvious precipitate-free zone and coarsen equilibrium phase are also presented in Figs.6(c) and (d). S' precipitates result in drastic reduction of free spacing for dislocation slip, which increases the effect of precipitation strengthening inside the grain, forces plastic deformation of the alloy to concentrate on PFZ at grain

boundaries and creates shearing deformation on PFZ to result in low plasticity. Moreover the coarse equilibrium particles (*S*) at grain boundary become the site for nucleation of crack. All of those are shown in Figs.3 and 4. Comparatively when aged for 20 min and 30 min, no PFZ and coarse particles of equilibrium phase (*S*) appear at grain boundaries (Figs.6(a) and (b)). The interior microstructure at that time is composed of dislocation cells and GP zones. Therefore the strength at grain boundaries is higher than that of the interior of grains, and the plastic deformation of samples mainly takes place in the interior of grains, which subsequently leads to a typical morphology of dimple-type of ductile fracture in tension test (Fig.3(a)).

As a result, the alloy exhibiting a ductile fracture when being aged for less than 40 min is due to the absence of PFZ adjacent to grain boundaries and the strength of grain boundaries higher than that of the interior of grain, resulting in plastic deformation mainly occurring within a grain. Moreover GP zone is shearable by dislocation slip and the size of dislocation cells is equal to free spacing of dislocation slip. The size of dislocation cells increase with aging time prolonging, followed by an aggrandizement of unstricted space of dislocation slip, so the elongation of tensile samples at this stage of ageing gradually increases. After being aged for 60 min, the reasons why the samples present a low ductility of fracture rest on two aspects as follows: one is that *S*′ precipitates obviously increase the effect of precipitation strengthening inside the grain, the other is that wide PFZ and coarse equilibrium phase becoming weak in alloy appear at grain boundaries. These two sides of effects mentioned above create a plastic deformation mainly at grain boundary and cracks easily nucleated at coarse equilibrium phases at grain boundaries. Therefore, a concentrated shearing plastic deformation occurs at grain boundaries and a low ductility of fracture appears in the sample of alloys.

4 Conclusions

1) The combined effects of strain hardening caused by high density of dislocation introduced by large cold rolled deformation and strengthening of GP zones precipitating at initial stage of ageing constitute the first peak of strength of 2024 aluminum alloy. The effect of strengthening led by the precipitation and growth of *S*′ phase that increase volume fraction of precipitates form the second peak of strength.

2) The decrease in the effect of strain hardening caused by introducing high density of dislocation in ageing process and followed by the increase in the effect of precipitation strengthening created by growth of *S*′ phase form two peak of strength in the ageing process of alloys, and present a characteristic of double peak of ageing strengthening.

3) The shearable characteristic of GP zone by dislocation slip and the absence of PFZ at early stage of aging result in a strength of grain boundary higher than that of the interior of grain and ductile fracture in subsequent tension test. The facts such as precipitation and growth of *S*′ phase, appearance of PFZ at grain boundary and coarsening of particles of equilibrium phase at grain boundary create a series of effects such as a strength of grain boundaries lower than interior of grain, cracks nucleated at coarse particles at grain boundaries and a concentrated shearing plastic deformation at grain boundaries, which forces the alloy to show a low ductility of fracture.

References

[1] DUCKWORTH W E. Thermomechanical treatment of metals [J]. JOM, 1966, 1: 915−922.

[2] MCEVILY A J, CLARK J B, BOND A P. Effect of thermal-mechanical processing on the fatigue and stress-corrosion properties of an Al-Zn-Mg alloy [J]. ASM Trans, 1967, 60: 661−671.

[3] RUSSO E D I, CONSERVA M, GATTO F, MARKUS H. Thermomechanical treatments on high strength Al-Zn-Mg(-Cu) alloys [J]. Metall Trans, 1973, 4(4): 1133−1144.

[4] OSTERMANN F. Improved fatigue resistance of Al-Zn-Mg-Cu(7075) alloys through thermomechanical processing [J]. Metall Trans, 1971, 2(10): 2897−2902.

[5] RUSSO E D I, CONSERVA M, BURATTI M, GATTO F. A new thermomechanical procedure for improving the ductility and toughness of Al-Zn-Mg-Cu alloys in the transverse directions [J]. Mater Sci Eng, 1974, 14: 23−36.

[6] RACK H J. The influence of prior strain upon precipitation in a high-purity 6061 aluminum alloy [J]. Mater Sci Eng, 1977, 29: 179−188.

[7] CHIA E H, STRARKE E A. Application of subgrain control to aluminum wire products [J]. Metall Trans, 1977, 8A(6): 825−832.

[8] JAHN M T, LUO J. Tensile and fatigue properties of a thermomechanically treated 7475 aluminum alloy [J]. J Mater Sci, 1988, 23: 4115−4120.

[9] WANHILL R J H, GESTEL G F J A V. Thermomechanical treatment of aluminum alloy [J]. Aluminum, 1978(9): 573−580.

[10] NOURBAKHSH S, NUTTING J. The high strain deformation of an aluminum −4% copper alloy in the supersatured and aged conditions [J]. Acta Metall, 1979, 28: 357−365.

[11] ZHANG Hong-zhe, ZHANG Yu-jie, ZHANG Xue-jun. Study of the thermomechanical treatment process and properties of aluminum alloy LD2 [J]. J Mater Sci Leters, 1993, 12(20): 1612−161.

[12] SINGH S, GOEL D B. Thermomechanical aging of 2014 aluminum. alloy for aerospace applications [J]. Bulletin of Mater Sci, 1991, 14(1): 35−41.

[13] DYMEKA S, DOLLAR M. TEM investigation of age-hardenable Al 2519 alloy subjected to stress corrosion cracking tests [J]. Mater Chem and Phys, 2003, 81: 286−288.

[14] TSUJI N, IWATA T, SATO M, FUJIMOTO S, MINAMINO Y. Aging behavior of ultrafine grained Al-2wt%Cu alloy severely deformed by accumulative roll bonding [J]. Sci and Tech of Adv Mater, 2004, 5: 173−180.

[15] RICHERT M, RICHERT J, ZASADZI´NSKI J, HAWRYŁKIEWICZ S, DŁUGOPOLSKI J. Effect of large

deformations on the microstructure of aluminium alloys [J]. Mater Chem and Phys, 2003, 81: 528−530.

[16] ZHENG L J, CHEN C Q, ZHOU T T, LIU P Y, ZENG M G. Structure and properties of ultrafine-grained Al-Zn-Mg-Cu and Al-Cu-Mg-Mn alloys fabricated by ECA pressing combined with thermal treatment [J]. Mater Character, 2003, 49: 455− 461.

[17] CHATURVEDI M C, CHUNG D W, DOUCETTE R A. Effect of thermomechanical treatment on structure and properties of 2036 aluminum alloy [J]. Met Sci, 1979(1): 53−57.

[18] SINGH S, GOEL D B. Influence of thermomechanical ageing on tensile properties of 2014 aluminum alloy [J]. J Mater Sci, 1990, 25: 3894−3900.

[19] ZHAO Gang, LI Hong-xiao, LIU Chun-ming, GUO Ya-ping. Thermomechanical ageing of 2014 aluminum alloy [J]. J Northeastern Univ(Natural Science Edition), 2001, 22(6): 664−667.

[20] CAROTENUTO G, GALLO A, NICOLAIS L. Degradation of SiC particles in aluminum-based composites [J]. J Mater Sci, 1994, 29: 4967−4974.

[21] VIALA J C, BOSSELET F, LAURENT V, LEPETICORPS Y. Mechanism and kinetics of the chemical interaction between liquid aluminum and silicon-carbide single crystals [J]. J Mater Sci, 1993, 28: 5301−5312.

[22] SANNINO A P, RACK H J. Effect of reinforcement size on age hardening of PM2009 Al-SiC 20vol% particulate composites [J]. J Mater Sci, 1995, 30: 4216−4322.

[23] SILCOCK J M. The structural aging characteristics of Al-Cu-Mg alloys with copper: magnesium weight ratios of 7:1 and 2.2:1 [J]. J Inst Metals, 1960, 61: 89, 203−210.

[24] GRIGORIS E K, STEFANOS M S, GEORGE A L. Aging response of aluminum alloy 2024/silicon carbide particles(SiC) composites [J]. Mater Sci Eng, 2004, A382: 351−361.

(Edited by YANG Bing)